Computational Bounds to the Quality Factor of a Fabry-Pérot Resonator Through Local Energy Conservation Laws

Simon Stone
Advisors: Prof. Owen D. Miller
Zeyu Kuang

Yale College, Class of 2021

May 2021

Abstract

In this paper, we identify computational bounds to the quality factor of a 1-dimensional Fabry-Pérot resonator. We do this by first analytically solving for the quasinormal modes of an open system, using the time-harmonic, source-free representation of Maxwell's equations. We then identify a complex frequency definition of the quality factor to make use in our optimization problem, which is formed through local power conservation laws embedded in Maxwell's equations. We identify a few distinct methods for choosing a "smart" selection of local power constraints, and using these methods we determine a tight upper bound to the quality factor of our system. The bound we identify is significantly tighter than previous analytical attempts at this 1D system.

Contents

1 Introduction **3**
- 1.1 Q-factor . . . 3
- 1.2 1D Fabry-Pérot Resonator . . . 4

2 Methodology **5**
- 2.1 Solving QNMs of 1D FP Resonator . . . 5
- 2.2 Complex Frequency Definition of Q-Factor . . . 5
- 2.3 Energy Conservation via Maxwell's Equations . . . 7
- 2.4 Formulation as a Maximization Problem . . . 7
- 2.5 Choosing Power Constraints . . . 9

3 Results **10**

4 Discussion **11**

5 Conclusion **13**

1 Introduction

Photonic and optoelectronic devices are well on their way towards disrupting electronic and communication industries across the globe. In the pursuit of optimizing such devices, the designer will often start by selecting physical parameters that best align with the intended device's behavior. With the emergence of computational sciences in the 21st century, computers have rapidly begun to replace the experimental method of physical design - instead of designing structures and performing tests in a laboratory environment, the "experiments" can instead be done on a computer, mitigating development costs and boosting production time. This becomes especially pertinent when considering nanostructures with dimensions on the order of the wavelength of light they interact with. The user can simply designate the performance characteristics of a device and an optimization algorithm will give the most favorable physical structure, without the additional costly and laborious fabrication process. The glaring issue here however, is that any design given by this computational process is not necessarily globally optimal, and may be missing better structures that have not been discovered. Performance bounds then can help the designer identify results of light-matter interactions that are possible or impossible in a complex design space [1]. This study will investigate computational methods for identifying such performance bounds.

1.1 Q-factor

One particular parameter of interest to engineers and scientists is the quality factor of a resonant system. Nanophotonic devices will often require the controlled localization of electromagnetic energy within a small region of space. If we want to minimize the energy loss in such a system, it is often prudent to use a quantity known as the quality factor. The quality factor, often abbreviated Q-factor or simply Q, is a dimensionless parameter that describes the lifetime of resonant energy in an oscillatory system.

There are many physical systems that can be described by the Quality factor, including acoustic systems, electrical systems (RLC circuits), and even a simple pendulum, but this study will limit its focus to resonant optical cavities. One example is that of a whispering gallery resonator, shown in *figure 1*. In this system, light is guided in a closed, circular path, and if upon each round trip the waves return to the same point with no phase difference, they will interfere with one another constructively, forming standing waves corresponding the resonant eigenmodes of the cavity. There are however, always associated loss mechanisms within any real resonator. In the case of an optical resonator, and for the duration of this paper, we consider absorption, scattering, and radiation losses that originate from intrinsic material properties and imperfections.

With these loss mechanisms in mind, we can begin to define the quality factor as the resonant frequency of the cavity, ω_0 times the ratio of the time averaged energy stored in the resonator, to the energy lost per cycle of oscillation:

$$Q = \omega_0 \frac{stored\ energy}{power\ loss} \tag{1}$$

Although this definition provides some insight regarding the physical interpretation of the Q-factor, it does little to help us formulate an optimization problem. To do this, we must first solve for the frequencies and mode profiles of the resonant system in question.

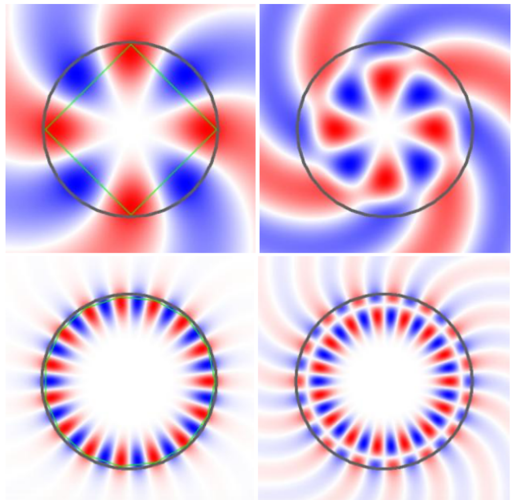

Figure 1: Eigenmode Profiles of Whispering Gallery Resonator. Green line (top left) represents geometrical ray path. Top row: modes of low Q with energy leaking into its surroundings. Bottom row: modes of high Q with energy more localized within the resonator

1.2 1D Fabry-Pérot Resonator

While the 2D case of the Whispering Gallery Resonator is certainly appealing, determining the mode profiles of such systems requires significant computational power. To better focus our efforts on computational bound methods, we instead use the case of a 1-dimensional Fabry-Pérot resonator. Such a system is formed by two parallel semi-reflecting surfaces and filled with a homogeneous medium of refractive index n. This resonator achieves resonance through the same mechanism as previously mentioned: incident waves will constructively interfere with circulating waves of the same phase, forming standing waves within the cavity. *Figure 2* provides a visual for this physical mechanism.

Before explicitly solving for the modes and frequencies of an FP resonator, we must first define the electromagnetic modes of an open system. Inevitably, due to the loss mechanisms previously mentioned as well as the partial reflectivity of the mirrors, some electromagnetic energy will be lost to the surrounding environment. From this assumption then, we may consider our system open - the fields are not strictly confined to the resonator and leak to the whole universe. Let us consider then such an open or "leaky" electromagnetic resonator that is initially excited for a small period of time and then left freely to evolve. The general solution to such a "damped" oscillator will be given by the sum of the resonant modes of the system along with an exponentially decaying envelope that is characteristic of the damping rate. From this interpretation, we can tell that the modes of a leaky cavity are simply time-harmonic fields, with an associated complex angular frequency [2]. Most literature refers to such modes as quasinormal modes (QNMs), which is the designation that will be used through the rest of this paper.

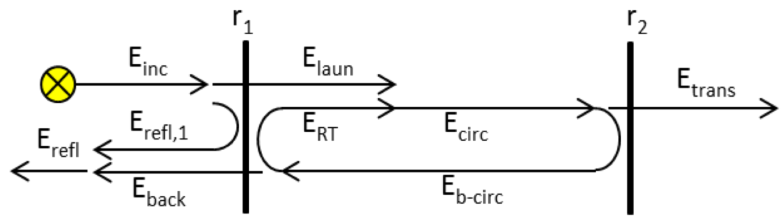

Figure 2: Schematic of FP-Resonator [3]

2 Methodology

2.1 Solving QNMs of 1D FP Resonator

To solve for our QNMs and associated resonant frequencies, we consider a 1D non-dispersive material material of length L. To find an analytical solution, we start with the frequency domain eigenproblem given by the time-harmonic source-free representation of Maxwell's equations:

$$\begin{bmatrix} 0 & i\epsilon^{-1}(\mathbf{z})\nabla\times \\ -i\mu^{-1}(\mathbf{z})\nabla\times & 0 \end{bmatrix} \begin{bmatrix} \tilde{\mathbf{E}}_m(\mathbf{z}) \\ \tilde{\mathbf{H}}_m(\mathbf{z}) \end{bmatrix} = \tilde{\omega}_m \begin{bmatrix} \tilde{\mathbf{E}}_m(\mathbf{z}) \\ \tilde{\mathbf{H}}_m(\mathbf{z}) \end{bmatrix} \tag{2}$$

where $\epsilon(\mathbf{z})$ and $\mu(\mathbf{z})$ are the position dependent permeability and permittivity of the system, respectively. Equation (2) is a non-Hermitian eigenproblem with eigenvectors corresponding to the field profiles and eigenvalues corresponding to the resonant frequencies. Given the scope of this problem, we can ignore the incident wave, and write field within the resonator as the superposition of two counter-propagating plane waves:

$$E(z) = Ae^{i\omega nz} \pm Ae^{-i\omega nz} \tag{3}$$

where $n = \sqrt{\epsilon}$ is the refractive index of the material, and A is the mode amplitude. We find that the resonant frequencies can then be solved quite easily:

$$\tilde{\omega}_m = \frac{\pi m}{nL} + i\frac{log(r)}{nL} \tag{4}$$

with the reflectivity of the mirrors given by $r = \frac{n-1}{n+1}$. This renders our problem far less computationally intensive than the 2D case, which likely would have required a series of rigorous numerical methods to solve for the eigenmodes and its associated eigenfrequencies.

2.2 Complex Frequency Definition of Q-Factor

Before proceeding with our optimization problem, we must first define the quality factor of our resonator in terms of the complex frequency using Poynting's theorem. We consider a singular quasinormal mode in our 1D space $(\tilde{\mathbf{E}}_m, \tilde{\mathbf{H}}_m, \tilde{\omega}_m)$. If we conjugate our equations for a source-free, time-harmonic electromagnetic field, we find that $(\tilde{\mathbf{E}}^*_m, \tilde{\mathbf{H}}^*_m, -\tilde{\omega}^*_m)$ is another perfectly valid solution with an equivalent Poynting vector. If we then apply the divergence theorem to our Poynting vector

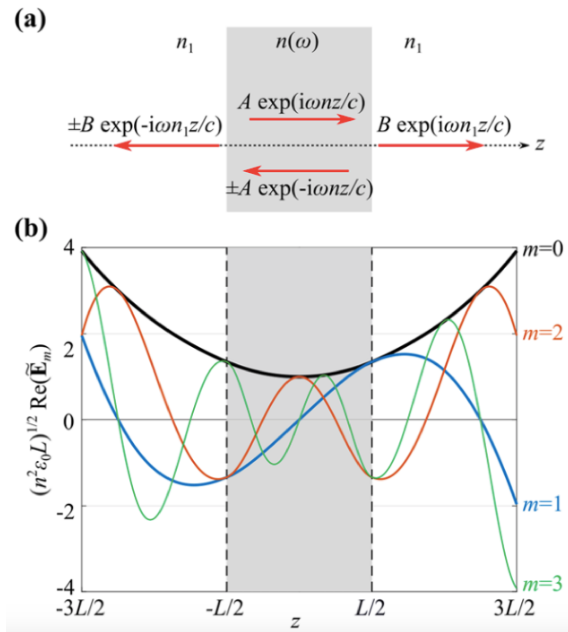

Figure 3: a) Plane wave representation of QNM in 1D FP Cavity. b) QNM Field Distribution of 1D FP cavity of length L [2]

over an arbitrary closed surface, we arrive at the following relation:

$$\begin{aligned}\frac{1}{2}\iint_S \Re(\tilde{\mathbf{E}}_m \times \tilde{\mathbf{H}}^*_m)d\mathbf{S} + \frac{\omega_m}{2}\iiint_V [\Im(\epsilon)|\tilde{\mathbf{E}}_m|^2 + \Im(\mu)|\tilde{\mathbf{H}}_m|^2]dV \\ = \frac{\omega_i}{2}\iiint_V [\Re(\epsilon)|\tilde{\mathbf{E}}_m|^2 + \Re(\mu)|\tilde{\mathbf{H}}_m|^2]dV\end{aligned} \tag{5}$$

where ω_r and ω_i are the real and imaginary parts of the resonant frequency, respectively. While this equation is certainly intricate, it offers some useful insights regarding power conservation in our system. We can readily see that the left hand side of equation (5) corresponds to the sum of radiated and absorbed power, while the right hand side corresponds to the time-averaged electromagnetic energy stored in the resonator. Following this interpretation of equation (5), as well the energy definition of the Q-factor from equation (1), we arrive at the following:

$$Q_m = -\frac{\Re(\tilde{\omega}_m)}{2\Im(\tilde{\omega}_m)} \tag{6}$$

This is the complex frequency definition for the Quality Factor, which we will use to define our optimization problem.

2.3 Energy Conservation via Maxwell's Equations

Any optimization problem will always require constraints. In the case of maximizing the Q-factor of a resonant electromagnetic system, the constraints we use are power conservation laws derived directly from Maxwell's equations. Similar to our derivation of the complex frequency Q-factor from section 2.2, we formulate Maxwell's equations with volume integrals. The difference here however, is that we separate the total field into its incident and scattered components. We also define the scattered field using the free-space Green's function, G_0, and the total field within the resonator using the induced polarization current $p(\mathbf{z})$, and the material susceptibility, χ.

Beginning with energy conservation, we know that the incident power must be equal to the sum of the scattered and absorbed power. Again, since we are dealing with a mode problem, we let the incident field be zero, letting us know that *scattered power* + *absorbed power* = 0. We also know that the induced polarization current within the resonator is directly related to the power by the system. Since this must be true at each point $\mathbf{z}$ in our complex design space, we can express this as a volume integral:

$$\int_V p^\dagger(\mathbf{z}) e_{scat}(\mathbf{z}) dV + [-\int_V p^\dagger(\mathbf{z}) e_{abs}(\mathbf{z})] = 0$$

or in matrix-vector notation:

$$p^\dagger(\mathbf{z}) e_{scat}(\mathbf{z}) + [-p^\dagger(\mathbf{z}) e_{abs}(\mathbf{z})] = 0$$

Using this relationship, and introducing a new term $\xi = \chi^{-1}$, we can arrive at the standard volume-integral-equation (VIE) over our design space:

$$[G_0 + \xi]p = 0$$

Finally, to find the conservation laws, we multiply this expression by a diagonal, complex operator $\mathbb{D}$, which will serve to identify our constraints. Taking the inner product of that results with ωp, we arrive at the final form of our N conservation laws [4]

$$p^\dagger \Re(\mathbb{D}_i[\omega^* G_0(\omega) + \omega^* \xi(\omega)])p = 0, \qquad i = 1, ..., N \tag{7}$$

The conservation laws of equation (7) satisfy two properties that are significant to our optimization problem. First, if we identify the operators G_0, ξ, and $\mathbb{D}$ over the entire computational design region V, the polarization current solutions correspond not just to V, but to *all* sub-domains of V, allowing global bounds over all possible designs [4]. A schematic demonstrating this property is shown in figure 4. The other important property is that the the $\mathbb{D}$-matrices themselves that we impose are quadratic, rendering the constraints susceptible to semidefinite programming, as discussed in later sections.

2.4 Formulation as a Maximization Problem

Identifying the upper bound of the quality factor requires that we maximize some particular metric subject to the previously defined constraints. Our goal is to do this over the space of all possible designs, therefore rendering the problem nonconvex and difficult to solve globally. Previous attempts to determine 1D upper bounds globally have ultimately been very loose (see figure 5), and so our end goal is to tighten the bound as much as possible. To achieve this, we employ constraints that correspond to both global *and* local conservation laws, such as those defined in equation (7). All

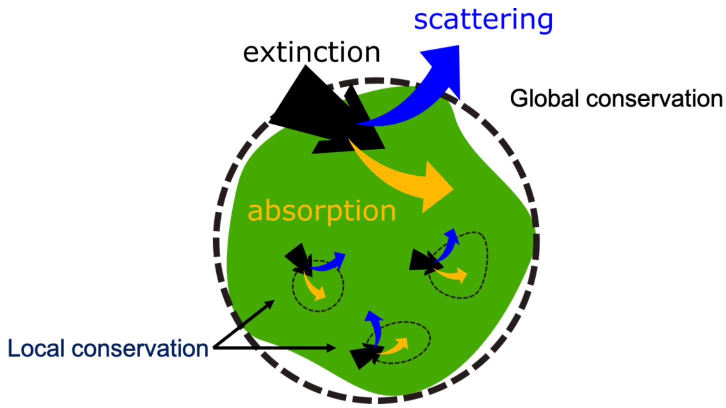

Figure 4: Global and local power conservation over an arbitrary design space [4]

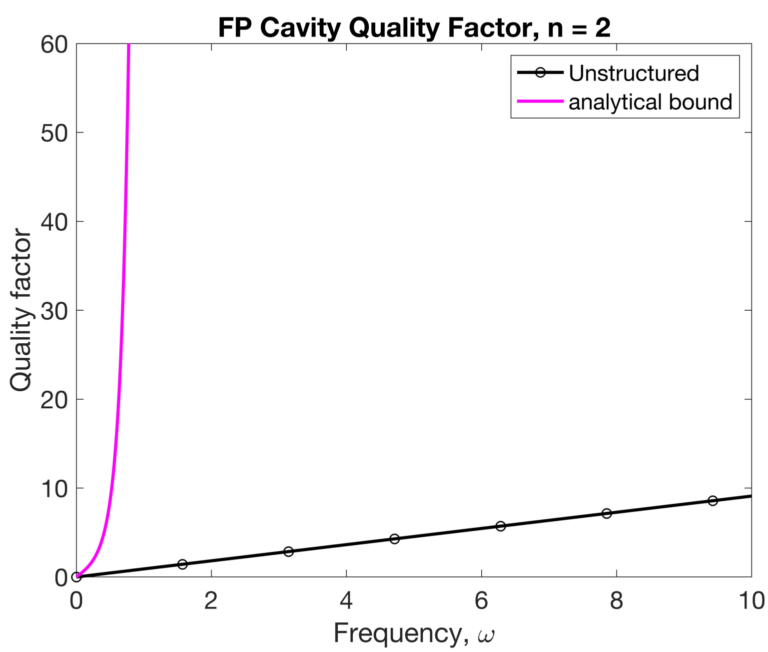

Figure 5: Loose Analytical Q Bound from a 2013 study by Osting and Weinstein. The looseness of the bound renders it unfavorable for any practical photonic design problem. [5]

that is left is to define the objective function of the optimization problem. Given the definition of the Q-factor from equation (7), it is apparent that we ought to minimize the absolute value of $\Im(\omega)$ in order to maximize Q. The maximal $\Im(\omega)$ then is given by the optimization problem:

$$\begin{aligned} \max_{p,\Im(\omega)} \quad & \Im(\omega) = -p^\dagger \Im(\omega^* G_0(\omega))p + p^\dagger \Im(\xi(\omega))p \\ \text{s.t.} \quad & p^\dagger \Re(\mathbb{D}_i[\omega^* G_0(\omega) + \omega^* \xi(\omega)])p = 0, \qquad i = 1, ..., N \\ & p^\dagger p = \Re(\xi) \end{aligned} \tag{8}$$

Equation (8) allows us to express this maximization problem as what is known as a quadratically constrained quadratic program (QCQP). An upper bound on the solution to this equation can be found by standard computational techniques that, upon each iteration i, relax the original quadratic program over semidefinite matrices to a higher-dimensional linear program. This commonly known as a semidefinite program (SDP), which in this study we solve through an optimization software package, MOSEK [6, 1, 7].

2.5 Choosing Power Constraints

Now that the optimization problem has been defined, then next step is to choose *which* local conservation laws to impose. It is computationally impractical to choose a large number of $\mathbb{D}$-matrices, but it would also be unsuitable to oversimplify the problem and achieve a loose bound. To speed up the computational process and find the tightest possible bound, we employ a "smart" selection of $\mathbb{D}$-matrices. The first two of these constraints correspond to global power conservation, but the rest must be chosen locally. We opt for three distinct, albeit related, methods for selecting this "smart" selection of local power constraints. The first and most effective method requires the selection of of the $\mathbb{D}$-matrix "most violated" by the optimal polarization current:

$$\mathbb{D}_{N+1} = \omega diag[p_{opt} p_{opt}^\dagger (\xi + G_0)^\dagger] \tag{9}$$

where p_{opt} is the optimal polarization current corresponding to the N^{th} power constraint. We can easily solve for this parameter upon each iteration of the optimization program by finding the largest eigenvector of the SDP varaible $\mathbb{X}$ with a built-in MATLAB function,

```
[p_opt]=eigs(X,1)
```

.

The second method we employed used the SDP variable directly after optimization.

$$\mathbb{D}_{N+1} = diag[(\xi + G_0) * \mathbb{X}]$$

Finally, the third method employed $\mathbb{D}$-matrices with diagonal elements orthogonal to all previous $\mathbb{D}$-matrices:

$$\mathbb{D}_{N+1} = \frac{(I - P_N)\mathbb{C}^*}{\|(I - P_N)\mathbb{C}^*\|}$$

with $\mathbb{C} = \omega^*(\xi + G_0)p_{opt}p_{opt}^\dagger$ and $P_N = \sum_{i=1}^N \mathbb{D}_{ii}\mathbb{D}_{ii}^\dagger$ as a projection matrix that projects onto the space of all vectors formed by the diagonal elements of $\mathbb{D}$. The comparative results of these methods can be seen in figure 6. To run the program, the user inputs an "initial guess" of $\Im(\omega)$, along with the mode number m for determining the resonant frequency, the permittivity of the

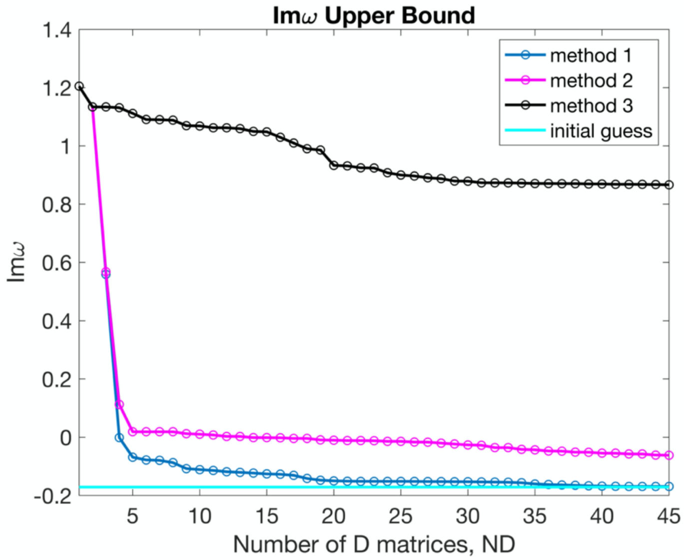

Figure 6: 3 different methods for choosing a "smart" selection of local power constraints. Method 1 converges the most rapidly to the initial guess of $\Im(\omega)$. In this example, $m = 4$.

resonator, the length of the design space, and the resolution of the design space. The program will then iteratively run an optimization for each number of imposed power constraints and return the maximum feasible value given those constraints. The more rapidly the maximum value converges, the tighter we know the bound can be. As seen in figure 6, the best bound enabling constraints are those corresponding to the optimal polarization current.

The following excerpt shows the iterative technique implemented in MATLAB:

```
for i = 3:ND
    einc = zeros(size(G0,1),1);
    D{i} = get_Dopt(popt{i-1},S,einc);
    [fmax(i),popt{i}] = bound_Ds(S,D,A,epsr,U);
    fprintf(' D matrix: %d / %d, fmax = %s \n', i, ND, fmax(i))
end
```

3 Results

Choosing only those constraints most violated by the optimal polarization current proved to be an effective method for calculating the upper bound of the Q-factor in 1D FP-resonator. As can be seen in figure 7, the method shows bounds significantly tighter than any previous result, and enabled the computation of up to 3 whole wavelengths within the resonator. The tightest bound was achieved solely through global power constraints, although our method of local power conservation agreed with the global bound quite well. As we increase the frequency it becomes ever more difficult to achieve as tight a bound, despite the fact that we increase the resolution of the design space. We

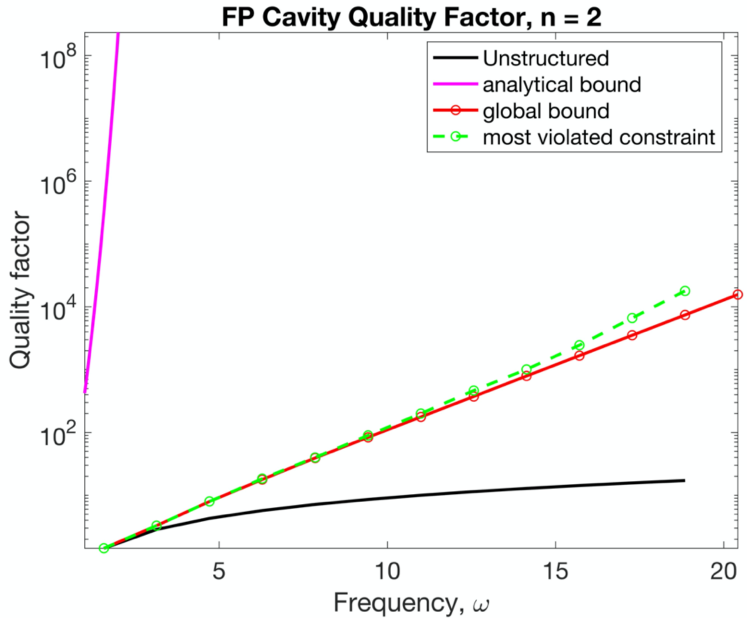

Figure 7: Upper bounds to the Q-factor of a 1D FP-Resonator. Computational bounds are significantly tighter than the previously calculated analytical bounds by a factor of roughly 10^5 [5].

also note that at high frequencies, the computation time increased dramatically, with the longest calculation taking roughly 6 hours.

4 Discussion

The local conservation laws derived in this paper from Maxwell's equations have been shown to enable computational upper bounds to the Q-factor of a 1D Fabry-Pérot Resonator. Our results are notably tighter than previous calculations, which allows for engineers and scientists to better understand the fundamental limits to their devices during the design process.

For example, consider the case of a series of whispering gallery resonators that are coupled to one another. One particular goal here might be to minimize scattering and absorption. By determining a tight upper bound to the Q-factor of each resonator, we can capture the degree to which this absorption and scattering can be reduced, resulting strong coupling as well as ultrahigh Q's (figure 8).

The next logical step in the development of this study would be to investigate an inverse design problem. Generally speaking, this type of design requires inputting the desired metrics to optimize into an algorithm, which will in turn provide the optimal structure. In the case of maximizing the Q-factor of a 1D Fabry-Pérot resonator, we would have an objective function of the form

$$f \sim Qe^{-(\omega-\omega_0)^2} \tag{10}$$

The intended algorithm would return a vector that maximizes the Q-factor given a target resonant

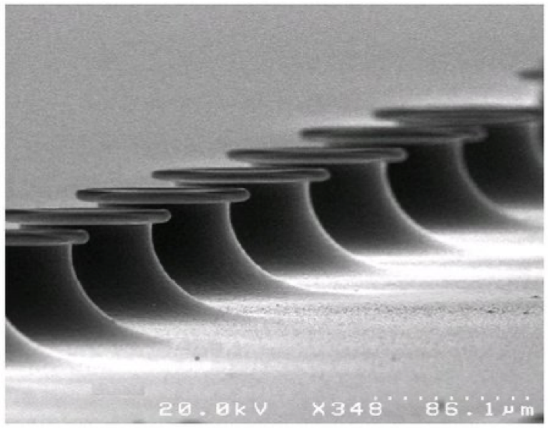

Figure 8: Array of Ultrahigh Q Microtoids [8].

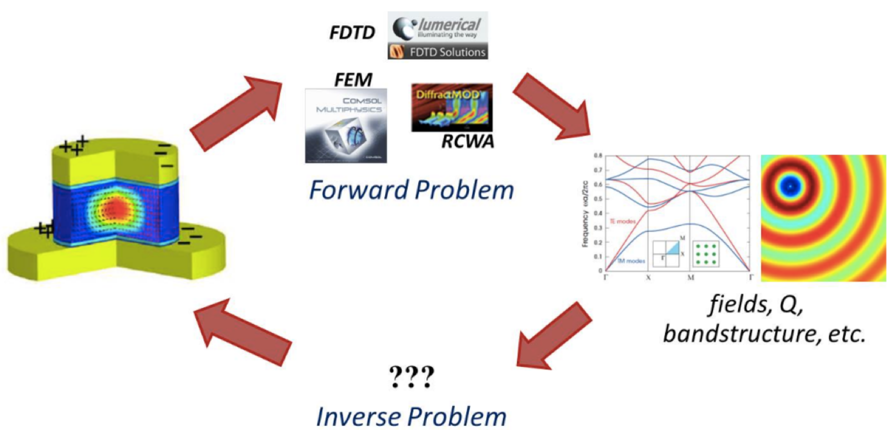

Figure 9: Inverse Design Problem [9].

frequency. The vector would have to contain the ordered information of the refractive indices in such a system, hence giving us the 1-dimensional geometry that optimizes such a resonator.

5 Conclusion

We have shown that tight computational bounds to the Q-factor of a 1D Fabry-Pérot resonator are possible through Maxwell-derived local conservation laws. We treat the modes of the resonator as quasinormal, allowing us to form analytical solutions for resonant frequencies and enabling faster computation times than the 2D case. The bounds we derive here have a slew of applications including integrate photonic circuit design, laser resonators, and even fiber optic communication. We also identify the subsequent practical work that can be built upon this study, namely, inverse design.

References

[1] Guillermo Angeris, Jelena Vučković, and Stephen Boyd. "Heuristic methods and performance bounds for photonic design". In: *Optics Express* 29.2 (Jan. 18, 2021), p. 2827. ISSN: 1094-4087. DOI: 10.1364/OE.415052. URL: https://www.osapublishing.org/abstract.cfm?URI=oe-29-2-2827 (visited on 05/15/2021).

[2] Philippe Lalanne et al. "Light Interaction with Photonic and Plasmonic Resonances". In: *Laser & Photonics Reviews* 12.5 (May 2018), p. 1700113. ISSN: 18638880. DOI: 10.1002/lpor.201700113. URL: http://doi.wiley.com/10.1002/lpor.201700113 (visited on 05/15/2021).

[3] Nur Ismail et al. "Fabry-Pérot resonator: spectral line shapes, generic and related Airy distributions, linewidths, finesses, and performance at low or frequency-dependent reflectivity". In: *Optics Express* 24.15 (July 25, 2016), p. 16366. ISSN: 1094-4087. DOI: 10.1364/OE.24.016366. URL: https://www.osapublishing.org/abstract.cfm?URI=oe-24-15-16366 (visited on 05/15/2021).

[4] Zeyu Kuang and Owen D. Miller. "Computational Bounds to Light–Matter Interactions via Local Conservation Laws". In: *Physical Review Letters* 125.26 (Dec. 31, 2020), p. 263607. ISSN: 0031-9007, 1079-7114. DOI: 10.1103/PhysRevLett.125.263607. URL: https://link.aps.org/doi/10.1103/PhysRevLett.125.263607 (visited on 05/15/2021).

[5] Braxton Osting and Michael I. Weinstein. "Long-Lived Scattering Resonances and Bragg Structures". In: *SIAM Journal on Applied Mathematics* 73.2 (Jan. 2013), pp. 827–852. ISSN: 0036-1399, 1095-712X. DOI: 10.1137/110856228. URL: http://epubs.siam.org/doi/10.1137/110856228 (visited on 05/15/2021).

[6] Zhi-quan Luo et al. "Semidefinite Relaxation of Quadratic Optimization Problems". In: *IEEE Signal Processing Magazine* 27.3 (May 2010), pp. 20–34. ISSN: 1053-5888. DOI: 10.1109/MSP.2010.936019. URL: http://ieeexplore.ieee.org/document/5447068/ (visited on 05/15/2021).

[7] Stephen P. Boyd and Lieven Vandenberghe. *Convex optimization*. Cambridge, UK ; New York: Cambridge University Press, 2004. 716 pp. ISBN: 978-0-521-83378-3.

[8] *UHQ Resonators: Background*. Vahala Research Group. URL: http://vahala.caltech.edu/research/uhq/highq (visited on 05/15/2021).

[9] Owen Dennis Miller. "Photonic Design: From Fundamental Solar Cell Physics to Computational Inverse Design". In: (), p. 137.